Research Article

Imidazolium-based ionic liquid silica xerogel as catalyst to transform CO_2 into cyclic carbonate

Daniela M. Rodrigues[1] · Leonardo M. dos Santos[2] · Franciele L. Bernard[2] · Ingrid S. Pinto[2] · Rubia Zampiva[3] · Gabriel Kaufmann[3] · Sandra Einloft[1,2]

Received: 11 August 2020 / Accepted: 14 October 2020 / Published online: 2 November 2020

Abstract
In this work silica xerogel samples containing different imidazolium ILs (EMIM-CF_3SO_3, EMIM-MSO_3, BMIM-Cl, MBMIM-TF_2N, BMIM-TF_2N and EMIM-TF_2N) were synthesized, characterized and used as catalyst in cyclic carbonate synthesis. ILs mass percentage was varied from 5% to 25%. The effect fostered by the ILs mass variation in the synthesis of silica xerogel was observed both in the materials characterization as well as in the performance of these materials as solid catalysts in the cyclic carbonate synthesis from the cycloaddition reaction of CO_2 with propylene epoxide. The obtained silica xerogel samples (SXs) were characterized by FTIR, RAMAN, TGA, SEM and TEM. The selectivity of the cycloaddition reaction was analyzed by GC and ^1H and ^{13}C NMR. The best results were obtained for SX-EMIM MSO_3 (20% of IL) and SX-BMIM Cl (15% of IL) with propylene carbonate yields of 91.4% and 83.4% and selectivities >99% and 97.4% respectively.

Keywords Xerogel silica · Ionic liquid · Catalyst · CO_2 · Cyclic carbonates · Cycloaddition reaction

1 Introduction

Carbon dioxide (CO_2) is one of the main greenhouse gases being emitted in large quantities. The anthropogenic burning of fossil fuels in the last decades is responsible for more than 60% of global warming [1–4]. On the other hand, CO_2 is also an interesting carbon source for synthesizing valuable chemicals and fuels [2, 5]. CO_2 chemical transformation into cyclic carbonates is interesting from a green chemistry point of view providing waste reuse, using safe reagents besides being a process with 100% CO_2 atom savings [6, 7]. Cyclic carbonates such as propylene carbonate (PC) find a wide application spectrum. PC can be used as intermediate in fine chemical production, pharmaceutical, and cosmetic industry, as secondary battery electrolytes, polar aprotic solvent as well starting material for polycarbonate production [6, 8, 9].

The disadvantage associated with using CO_2 as a starting reagent is its high thermal and kinetic stability, making it essential to use catalysts in the CO_2 chemical transformation reactions under milder reaction conditions [7, 10]. However, even using catalysts to overcome the high energy barriers for these reactions, high temperatures and CO_2 pressures are still necessary for these reactions to happen, resulting in high energy costs [10–18]. So, catalysts development and catalytic systems that are capable of transforming CO_2 into cyclic carbonates at temperatures below 100 °C and atmospheric CO_2 pressure are crucial reducing synthesis energy costs. Although some catalysts have already shown promising results, they are still considered expensive and difficult to apply on an industrial scale, making it important to search for new materials that combine mild reaction conditions, low production costs and applicability on an industrial scale [19–26].

✉ Sandra Einloft, einloft@pucrs.com.br | [1]Post-Graduation Program in Materials Engineering and Technology, Pontifical Catholic University of Rio Grande do Sul – PUCRS, Porto Alegre, Brazil. [2]School of Technology, Pontifical Catholic University of Rio Grande do Sul PUCRS, Porto Alegre, Brazil. [3]Graduate Program in Mining, Metallurgical and Materials Engineering, PPGE3M, Federal University of Rio Grande do Sul-UFRGS, Porto Alegre, Brazil.

Several homogeneous catalytic systems have already been efficiently established for these syntheses [27–32]. However, the high cost and difficulty related to catalyst/product separation, catalyst recycling and synthesis intensified the search and use of heterogeneous catalytic systems [33].

Ionic liquids (ILs) are already widely reported in literature as homogeneous catalysts presenting high catalytic activity and selectivity in cyclic carbonate synthesis [28, 30]. Yet, they are considered environmentally friendly catalysts and solvents due to their characteristics such as low vapor pressure and toxicity, good thermal stability and high synthetic versatility [27, 33, 34]. In this way, the search for new options to overcome the intrinsic disadvantages of homogeneous catalysts is imperative. ILs supported or immobilized on different materials such as natural or synthetic polymers, silica, zeolite, clays, among others, appears as promising heterogeneous catalysts to epoxide CO_2 cycloaddition reactions [33–36]. In the last decades, several studies have reported the synthesis of aerogels and xerogels containing ionic liquids. These materials can be applied as support and enzymatic immobilizers [37], catalyst support [35, 38], auxiliary materials for nanoparticle formation [39], molds for nanoporous and inorganic mesoporous materials preparation [38, 40, 41], and drug removal from wastewater [42]. In previous work, our group reported the synthesis of silica xerogels containing ILs for use in CO_2 sorption and CH_4/CO_2 separation [43].

In this work we investigated the catalytic behavior of silica xerogels (SX) containing the EMIM CF_3SO_3, EMIM MSO_3, BMIM Cl, MBMIM TF_2N, BMIM TF_2N, and EMIM TF_2N ionic liquids in cycloaddition reactions of CO_2 with propylene epoxide. Different concentrations of EMIM MSO_3 and BMIM Cl were analyzed and the influence of combining different structures of cations and anions of these ILs was investigated as well.

2 Materials and methods

For the SX-ILs synthesis, the following precursors were used: Tetraethylorthosilicate (TEOS, 98%, Merck), Sodium Fluoride (NaF, 99% Synth), Polyvinyl Alcohol (PVA, 194.5%, Dynamics, Brazil), Hydrochloric acid (HCl, 36.8%, Anhydrol), Acetone (99.5%, Vetec) and 1-ethyl-3-methylimidazolium methanesulfonate (EMIM-MSO_3, 95%, Merck). The IL EMIM MSO_3 was used as received. The IL BMIM Cl were synthesized according to the procedures reported in literature [44]. The characterizations of these ILs were performed using nuclear magnetic resonance spectroscopy (^{1}H NMR) analysis on Varian spectrophotometer; model VNMRS 300 MHz, using DMSO as solvent (d6, 25 °C). BMIM Cl ^{1}H NMR (300 MHz, DMSO-d6, 25 °C), δ (ppm):1.01 (m, CH_3), 1.29 (m, CH_2CH_3), 1.83 (m, CH_2), 3.97 (s, CH_3), 4.25 (t, CH_2 N), 7.79 (s, H5), 7.91 (s, H(4)), 9.48 (s, H(2)).

For carbonates synthesis and characterization, propylene oxide (PO, 99%, Sigma Aldrich), epiclorohydrin (99%, Sigma Aldrich), 1,2-epoxybutane (99%, Sigma Aldrich), ethyl ether (99.0%, Vetec), carbon dioxide (CO_2, 99.998%, White Martins), and propylene carbonate (99.0%, Alpha Aesar) were used as received.

2.1 SX-ILs synthesis

SX containing different amounts of ILs BMIM Cl and EMIM MSO_3 were synthesized following procedures described in the literature [43]. Firstly, 2.28 mmol of TEOS, PVA (4.64 g/L), NaF (0.20 g/L), 6.86 mmol of distilled water, and different amounts of ILs (25 mg to 150 mg) were mixed. The reaction mixture was stirred and brought to the freezer until gelation. The obtained gels were kept at 35 °C for 24 h and washed several times with acetone and n-pentane. Finally, the silica xerogels were dried at 35 °C for 24 h. A sample of silica xerogel (SX) was also prepared without IL. The silica xerogels containing ILs were labeled SX-IL N. Where N ranges from 1 to 4, and each unit corresponds to the addition of an additional of 5% of IL to the silica xerogels. For example, SX-BMIM Cl 1 corresponds to silica xerogel containing 5% of 1-butyl-3-methylimidazole chloride and SX-BMIM Cl 4 to SX containing 20% 1-butyl-3 chloride methylimidazole.

The syntheses of xerogels containing 5% of ionic liquid (SX-BMIM TF_2N 1, SX-EMIM CF_3SO_3 1, SX-mBMIM TF_2N 1, and SX-EMIM TF_2N 1) have already been described in a study previously published by our group as sorbents for CO_2 sorption and CH_4/CO_2 separation [43]. SX-BMIM Cl 1 and SX-EMIM $MSO_3$1 presented good behavior as catalysts in the cycloaddition reactions of CO_2 with propylene oxide. Therefore, in this work, SX-BMIM-Cl and SX-EMIM MSO_3 containing different ILs concentrations will be produced as indicated in Table 1.

2.2 SX-ILs characterization

SX-BMIM-Cl N and SX-EMIM-MSO_3N will be chemically, morphologically, and structurally characterized and their behavior as catalysts in cycloaddition reactions of CO_2 with propylene oxide will be compared to the SX-IL N previously described by our group [43].

SXs structure investigations were performed by Fourier transform infrared spectroscopy (FTIR) analysis using a Perkin-Elmer model Spectrum 100 FT-IR spectrometer using KBr pellets in the range of 4000 to 500 cm^{-1}. The ^{13}C MAS and ^{29}Si MAS NMR spectra were obtained using Bruker advance III HD 400 MHz spectrometer. SX-ILs thermal decomposition behavior and the quantification of IL

Table 1 Catalytic performance of SX IL N

Entry	Catalyst	Pressure/CO_2 (bar)	Conversion (%)	Selectivity (%)[e]	Yield (%)
1	EMIM MSO_3[a]	40	3.5	–	–
2	BMIM-Cl[b]	40	64.4	95.8	61.7
3	SX-Pristine	40	7.9	–	–
4	SX-BMIM NtF_2 1	40	16.8	98.9	16.6
5	SX-EMIM CF_3SO_3 1	40	20.5	64.8	13.3
6	SX-mBMIM NtF2 1	40	16.4	95.4	15.6
7	SX-EMIM NtF2 1	40	21.1	92.2	19.5
8	SX-EMIM MSO_3 1	40	26.3	93.3	24.5
9	SX-EMIM MSO_3 2	40	62.0	94.7	58.7
10	SX-EMIM MSO_3 3	40	84.9	>99.9	84.0
11	SX-EMIM MSO_3 4	40	92.3	>99.9	91.4
12	SX-EMIM MSO_3 4	30	55.4	>99.9	54.8
13	SX-EMIM MSO_3 4	50	73.3	>99.9	72.6
14	SX-EMIM MSO_3 4[c]	40	49.0	81.7	40.0
15	SX-EMIM MSO_3 4[d]	40	75.7	>99.9	74.9
16	SX-BMIM Cl 1	40	39.7	93.7	37.2
17	SX-BMIM Cl 2	40	68.6	91.2	62.6
18	SX-BMIM Cl 3	40	85.5	97.6	83.4
19	SX-BMIM Cl 4	40	83.5	>99.9	82.6

[a]1.1 mmol of ILs

[b]0.9 mmol of ILs

[c]Temperature of 120 °C

[d]Temperature 100 °C

[e]The selectivity of the reactions was determined by GC. Catalyst XS-IL = 0.7 g; 110 °C; 6 h

incorporated to the SX was investigated by thermogravimetric analysis (TGA) using aSDT-Q600 instrument at a temperature range from 25 °C to 600 °C with a heating rate of 20 °C/min under nitrogen atmosphere. The amount of IL incorporated in the SX was calculated following the formula adapted from [45], (wt% $SX_{200–600\,°C}$ − wt% SX-IL $N_{200–600\,°C}$). The influence of the ILs concentration on the SX-ILs structure was analyzed by Raman spectroscopy in an inVia Renishaw Raman spectrometer equipped with a 532 nm laser. Samples morphology was determined with a field emission scanning electron microscope (FESEM) using Inspect F50 equipment (FEI Instruments) in secondary electrons mode and transmission electron microscopy (TEM) using a Tecnai G2 T20 FEI operating at 200 kV.

2.3 Cyclic Carbonate synthesis

PC synthesis was performed in a 120 mL titanium reactor by loading the reactor with 1.0 mol of epoxide and 0.8 g of SX-IL N. The reaction conditions were previously defined. CO_2 pressures and temperature were varied from 30 to 50 bar and 100 to 120 °C of temperature respectively. Reaction time was 6 h. All reactions were carried out solvent-free and after each reaction, the final product was filtered and the catalyst washed with acetone for complete separation of propylene carbonate/SX-ILs N.

Cyclic carbonate selectivities were performed by gas chromatography analysis using a Shimadzu GC-14B chromatograph, equipped with a flame ionization detector (FID) and a SH-Rtx-5 column (30 m × 25 mm × 25 mm). To determine selectivity, a direct quantitative analysis method was employed by preparing a series of standard solutions with concentrations from 1% to 5% of propylene carbonate used to construct a calibration curve. Nuclear magnetic resonance (^{1}H NMR) analysis was also performed on the reaction final product after it was separated by filtration of the SX-IL catalyst to verify if remnants of the ILs had been leached from the SXs reinforcing the selectivity of the reaction. The ^{1}H NMR analysis was performed on Varian Spectrophotometer, model VNMRS 300 MHz, using $CDCl_3$ as solvent (d6, 25 °C).

Conversion of propylene carbonate was calculated by the difference in mass of the reactants and the final product (after the catalyst being separated by filtration and the remaining propylene oxide by vacuum and heating). Propylene carbonate conversion was calculated using Eq. (1).

$$Conv.(\%) = \frac{W_{PF}}{\frac{M_{Cx} \; X \; W_{Ox}}{M_{Ox}}} \quad (1)$$

where W_{PF} is the weight of the final product, MC_{cx} is the molar mass of the carbonate formed, W_{ox} is the weight of the oxide used and Mox the molar mass of the oxide used.

Reaction scaling is obtained by multiplying the reaction conversion by the selectivity obtained by the gas chromatography (GC) analysis of the product formed in the reaction.

3 Results and discussions

In this work, we will present the characterization of xerogels SX-BMIM Cl and SX-EMIM MSO_3 containing different ILs concentrations. These compounds worked very well as catalysts in cycloaddition reactions of CO_2 with propylene oxide. Xerogels containing 5% of ionic liquid (SX-BMIM TF_2N 1, SX-EMIM CF_3SO_3 1, SX-mBMIM TF_2N 1, SX-EMIM TF_2N 1, SX-EMIM MSO_3 1, and SX-BMIM Cl 1) are efficient materials for CO_2 capture and CO_2/CH_4 separation as previously published by our group [43].

3.1 Structural Analysis—(FTIR)

SX-BMIM Cl N and SX-EMIM MSO_3 N chemical structures investigation was performed by FTIR analysis. Figure 1 shows typical spectrograms of SX-ILs containing different IL concentrations. Condensed silica formation was confirmed by the presence of a broadband in the region from 1000 cm^{-1} to 1350 cm^{-1}as well as by the shoulder-shaped band in the region between the bands at 1079 cm^{-1} and 1199 cm^{-1} attributed to the asymmetrical elongation vibration of siloxane (Si–O–Si) bridges [42, 46]. The bands at 790 cm^{-1} and 619 cm^{-1} are attributed to the v Si–O–Si symmetrical elongation vibration and the band at 949 cm^{-1} to the S–O bond oscillation indicating the successful silica network formation [40, 42, 46]. According to [46], the broadband in the region between 3650 and 2800 cm^{-1} can be attributed to the vibrational modes of asymmetric and symmetrical elongation of the residual and/or adsorbed water present in the samples, confirmed by the appearance of the band at 1639 cm^{-1} corresponding to the symmetrical flexion vibrations of the water. The presence of this broadband, related to the presence of water masks the presence of the band that should appear in the 3000 cm^{-1} regions corresponding to the C–H connection. The band in the region of 1460 cm^{-1} is attributed to the asymmetric elongation vibration of CH_3–N–C–N– present in the imidazole ring of the IL.

Increasing SX IL concentration increases the normalized area of the vCH_2–N– and CH_3–N– symmetric and asymmetric stretching, imidazole ring characteristic band. The obtained normalized areas were 0.27, 0.82, 1.38 and 2.7 for SX-EMIM MSO_3 1, SX-EMIM MSO_3 2, SX-EMIM MSO_3 3 and SX-EMIM MSO_3 4 respectively, as shown in Fig. 2.

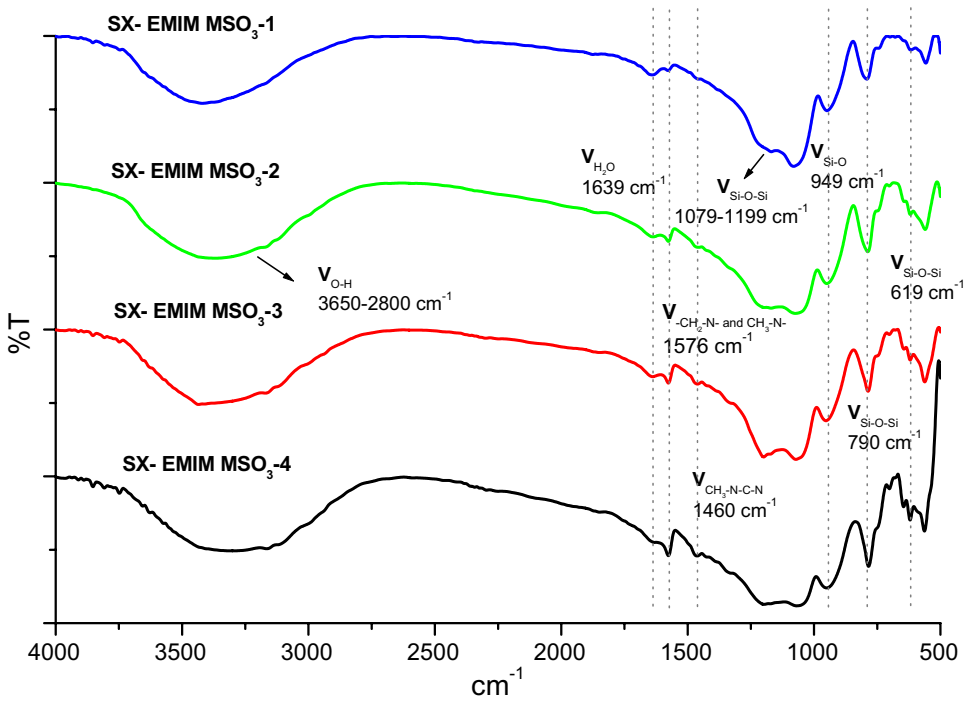

Fig. 1 FTIR of SX-EMIM MSO_3 1, 2, 3 and 4

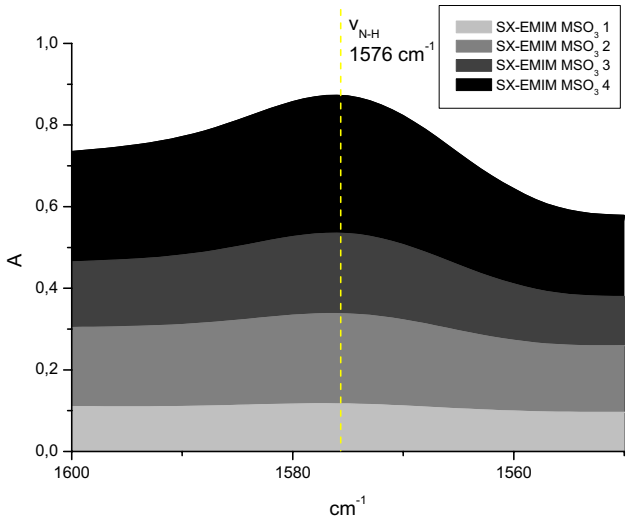

Fig. 2 IR spectrum with increasing bandwidth of the imidazole ring

3.2 Raman Spectroscopy and Solid-state ^{13}C and ^{29}Si NMR analyses

The conformation of different concentrations of BMIM Cl and EMIM MSO_3 confined within the mesoporous silica gel was characterized by Raman spectroscopy. Figure 3a and b present the normalized Raman spectra of BMIM Cl N and EMIM MSO_3 N respectively.

The Pure SX substrate presented elevated fluorescence almost completely covering the sample Raman signal. Only a single band is identified at 2426 cm^{-1}. With the IL insertion in the SX structure, the fluorescence decreases and bands in the 2800–3200 cm^{-1} range arise due to the presence of C–H deformation vibrations in the imidazolium ring and C–H stretching vibrations [47]. Because of the structural similarities between BMIM Cl and EMIM MSO_3 (Fig. 3c and d), both IL present bands in the 2800–3200 cm^{-1} range. A clear difference is observed

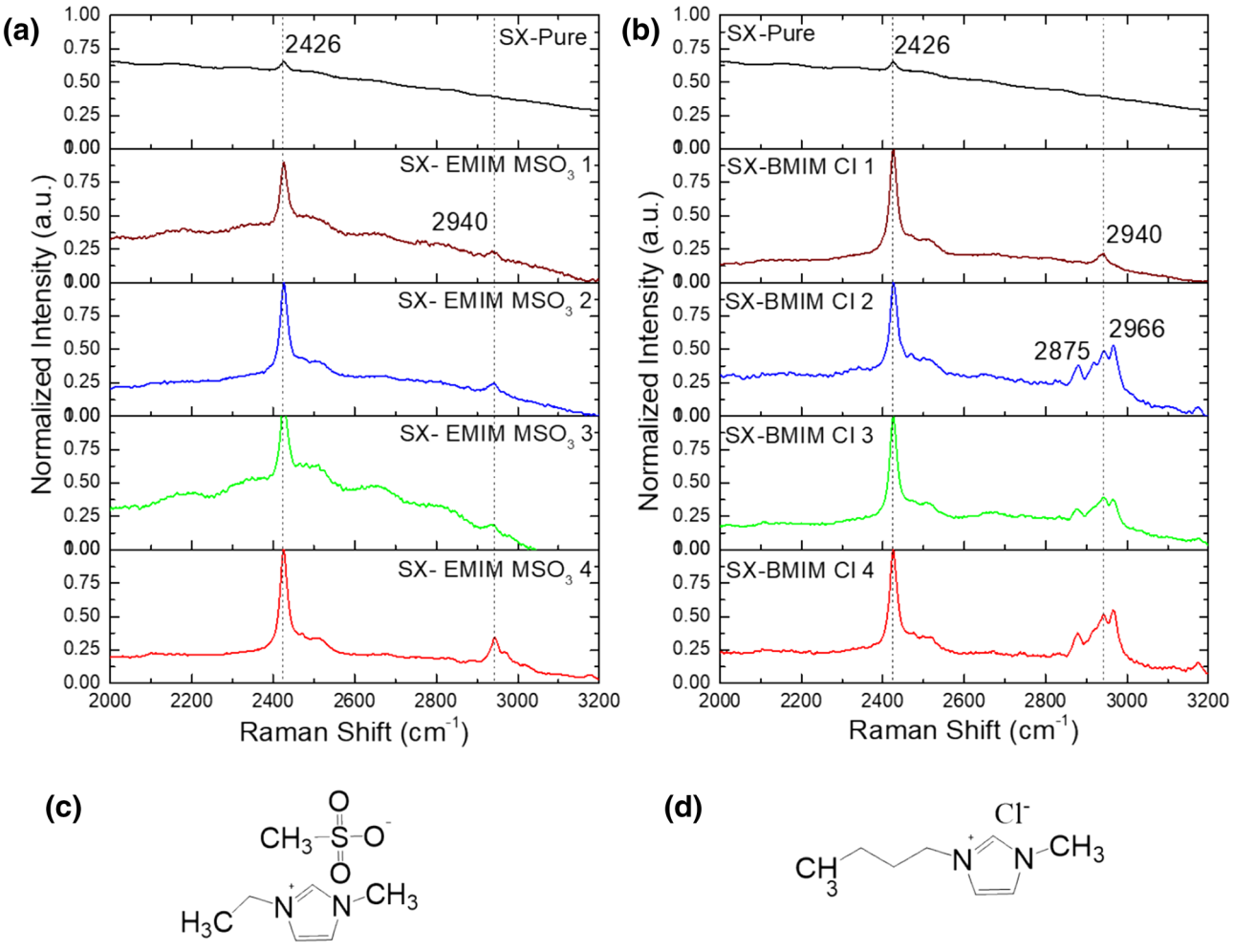

Fig. 3 Raman spectroscopy analyses of SX-EMIM MSO_3 N and SX-BMIM Cl N. (**a**) SX-EMIM MSO_3 N normalized spectra and (**b**) SX-BMIM Cl N normalized spectra. The chemical structure of EMIM MSO_3 and BMIM Cl are presented in (**c**) and (**d**) respectively

when comparing the SX-IL N spectra to the Pure SX that presents only one defined band at 2426 cm^{-1}.

NMR was used to evidence the incorporation of ionic liquid in silica xerogel using sample SX-EMIM MSO_3 4. In the ^{13}C CPMAS NMR spectrum of SX-EMIM MSO_3 4, the characteristic regions of silica xerogel, 15 (CH_3), 45 (OCH_2) ppm are observed. The signs indicating the presence of the IL are found in the regions of 37–40 (aliphatic chain) and 122–136 ppm (C of the aromatic ring). For the ^{29}Si CPMAS NMR analysis of the SX-EMIM MSO_3 4, three distinct siloxane resonance signals were observed in the Q2 regions at −91; Q3 at −101, and Q4 at −110 ppm. The spectra obtained for the other samples were previously reported in the study by dos Santos et al. [43].

3.3 Thermogravimetric analysis

Figure 4 presents a typical thermogram of the SX-IL N xerogels ($n = 1, 2, 3$ and 4) used in this work. For the SX-BMIM-Cl N xerogels samples (see Fig. 4), the first loss of mass (9.5 ± 1.5% to 12.2 ± 1.5%) occurs between 29 °C and 150 °C and corresponds to water and solvent organic evaporation [48]. The second mass loss (35.8 ± 1.5% to 14.2 ± 1.5%) observed occurs between 258 °C and 436 °C attributed to the decomposition of the IL BMIM Cl and/or PVA [49, 50].

The increase in the ILs concentration present in xerogels causes a decrease in inorganic compounds. By looking at the TGA thermograms in Fig. 4, one can see that the residual percentage decreases (from 70.2 ± 1.5% to 46.9 ± 1.5% for SX-BMIM Cl 1 and SX-BMIM Cl 4, respectively) with the increase of ILs concentration present in the xerogels [49–51]. IL BMIM Cl content incorporated into the SX matrix was determined from TGA. The values were

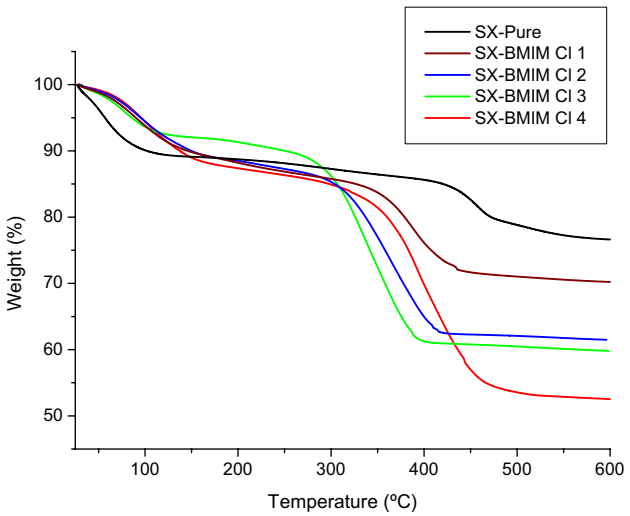

Fig. 4 Typical thermogravimetric analysis of the SX-IL's with the concentrations of ILs ranging from 5% to 20%

5.9 ± 1.5%, 8.8 ± 1.5%, 15.6 ± 1.5% and 22.9 ± 1.5% for SX-BMIM Cl 1, 2, 3 and 4 respectively.

3.4 Morphological Analysis (SEM/TEM)

Figure 5 presents SEM images of pristine silica xerogels as well as silica xerogels containing the ILs BMIM Cl Fig. 5a–d and EMIM MSO_3 Fig. 5e–h. As seen in Fig. 5i the xerogel synthesized without ILs addition presents a dense appearance due to gel shrinkage during the solvent evaporation step [52]. In xerogels synthesized with different concentrations of the ILs BMIM Cl and EMIM MSO_3 (a–h), agglomerated spheres that increase in size with the increasing concentration of IL contained in xerogels were formed. The variation in bead diameter was 0.137 µm to 6.404 µm for SX-BMIM Cl 1 and 4 respectively and 3.525 µm to 3.809 µm for SX-EMIM MSO_3 1 and 4, respectively. The presence of the ionic liquid is crucial in the aging/drying step of xerogels synthesis. In this step, the IL acts as a drying control agent, forming a less volatile film on the inner wall of these spheres formed by the silica network. The IL presences make it difficult for the spheres to collapse during solvent evaporation, avoiding shrinkage and formation of a dense structure as shown in Fig. 5i for pristine SX [40, 52, 53].

SX-EMIM MSO_3 4 TEM analysis provides additional evidence of IL confinement within the SX closed/isolated pores (compare Fig. 6a with Fig. 6b and c). Figures 5b, c, d, e, f and g 6d also shows the formation of open pores presenting a continuous channel of communication with sample external surface (d ~ 74 nm, indicated by yellow arrows) as described in literature [40, 52].

When comparing TEM images of samples SX-Pristine (Fig. 6a) and SX-EMIM MSO_3 4 (Fig. 6b, c and d) one can observe the formation of darker regions (compare Fig. 6a) with Fig. 6b, c and d) attributed to the IL confinement and also open pores in the SX structure (Indicated by yellow arrows) [40, 52, 54].

3.5 Synthesis of propylene carbonate

The catalytic performance of synthesized SXs is presented in Table 1. The reaction conditions were previously selected based on published studies using ionic liquids and supported ionic liquids as catalysts for cycloaddition reactions [27, 34, 36, 55]. Samples SXs containing 5% of ILs were tested (Table 1 entry 4–8 and 16) using a CO_2 pressure of 40 bar, temperature of 110 °C and a reaction time of 6 h. The yield in propylene carbonate were 16.6%, 13.3%, 15.6%, 19.5%, 24.5% and 37.2% (Table 1, entries 4–8 and 16, respectively). The highest catalytic activities were achieved by SX-BMIM Cl 1 and SX-EMIM MSO_3 1. In previous work, we described the CO_2 affinity for SXs samples [43]. The higher catalytic activity of SX-BMIM Cl 1 and

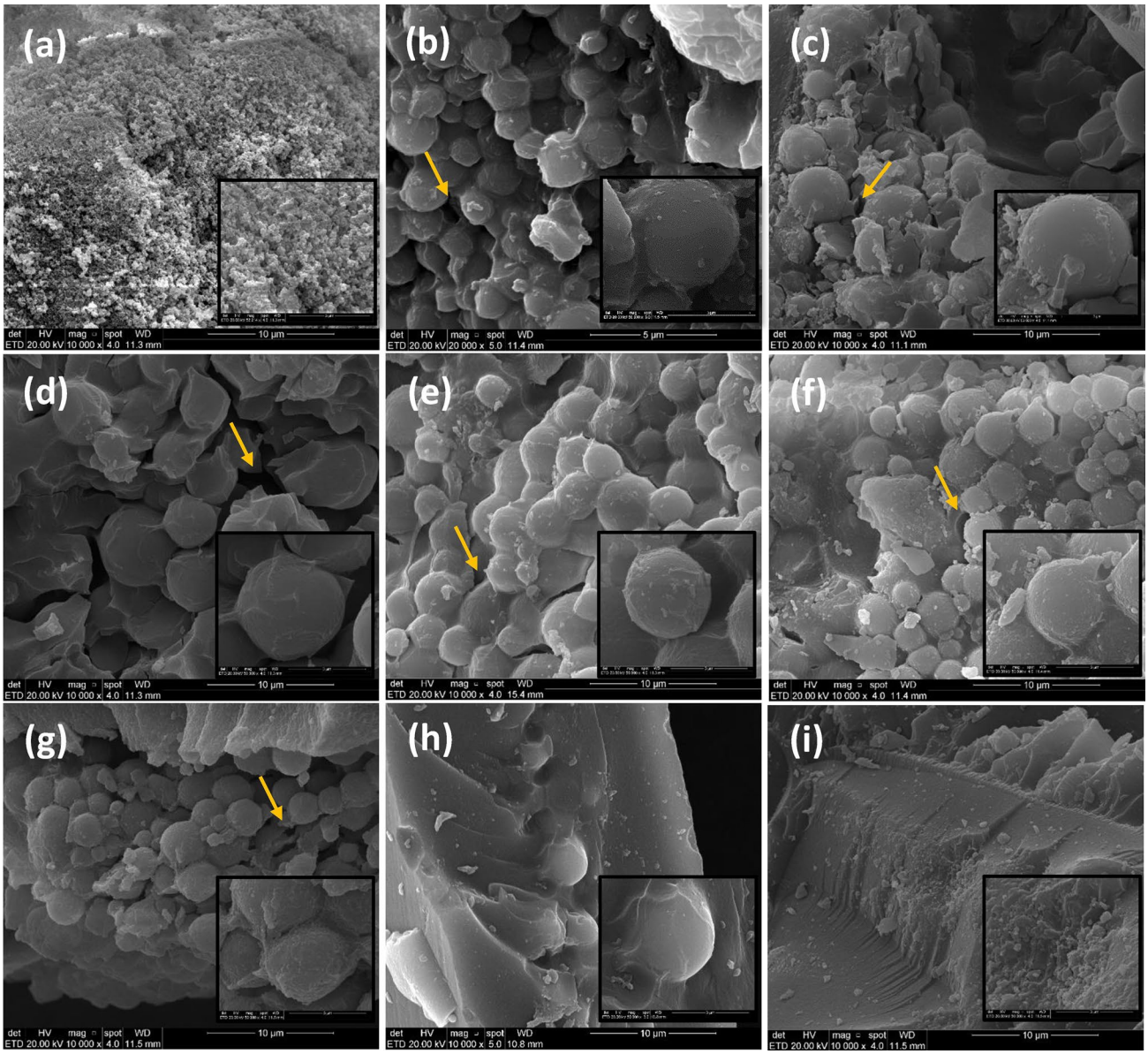

Fig. 5 SEM (**a**) SX-BMIM Cl 1, (**b**) SX-BMIM Cl 2 (**c**) SX-BMIM Cl 3, (**d**) SX-BMIM Cl 4, (**e**) SX- EMIM MSO_3 1, (**f**) SX- EMIM MSO_3 2, (**g**) SX-EMIM MSO_3 3, (**h**) SX-EMIM MSO_3 4 and (**i**) SX-pristine

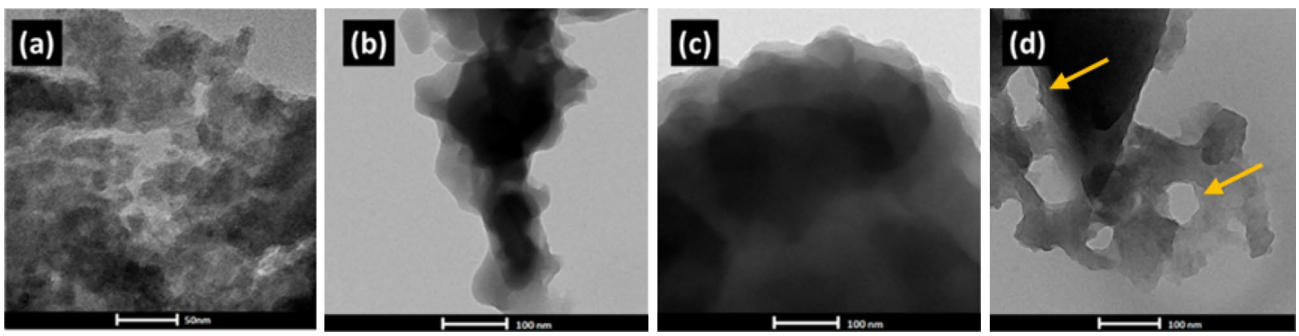

Fig. 6 TEM image of SX-pristine (**a**) and SX-EMIM MSO_3 4 (**b**, **c** and **d**)

SX-EMIM MSO_3 1 when compared to the other SXs samples tested as catalyst (see Table 1; entry 4–8 and 16) is probably related to the lower affinity for CO_2. Unlike for CO_2 capture the poor SXs/CO_2 interaction, in this case, facilitates the IL/epoxide interaction, and consequently the opening of the epoxide ring for subsequent CO_2 insertion and propylene carbonate formation [36]. Based on these results the SXs with the best catalytic activity (SX-BMIM Cl and SX-EMIM MSO_3) were elected to investigate the effect of the increase of ILs concentration on the SX synthesis on the catalytic activity of cycloaddition reactions. For SX-BMIM Cl, the increment of 5% in the ILs concentration (5%, 10%, 15% and 20%) causes a consecutive increase in product yield of 37.2%, 62.6%, 83.4%, and finally stabilizes at 82.6% (Table 1, entries 16, 17, 18 and 19, respectively). The increase in yield increasing the ILs concentration may be related to the ILs forming a thin layer, both in the SX pores and channels close to their surface causing an increase in the interaction of the ILs with the substrate. Yield stability when the concentration of ILs reaches 15% indicates the existence of a maximum concentration of ILs in the SX matrix that results in yield increment. An excess of IL could clog the porous silica network channels preventing the CO_2 or propylene oxide to access these channels [51]. Also, the excess of ILs in the synthesis of SXs could bring fragileness to the porous silica network [52, 56].

The SX-EMIM MSO_3 demonstrated the same trend presented by SX-BMIM Cl, but with better results for an increase in ILs concentration. The increase in ILs concentration up to 20% increased the yield of propylene carbonate of 24.5%, 58.7%, 84.0%, and 91.4% (Table 1, entries 8, 10, 11, and 12, respectively). However, when the ILs concentration was increased to 25% the propylene carbonate yield dropped by almost half (48.5%), corroborating the existence of a maximum amount of ILs used in the SXs synthesis that results in yield increase. Subsequently, the SX-EMIM MSO3 4 was elected to study the influence of temperature and pressure (Table 1, entries 12–13 and 14–15, respectively). Both the increase and the decrease in temperature cause a sharp drop in the reaction yield evidencing that the temperature has a great influence on the PC yield. The same behavior was observed for pressure being the best reaction conditions for PC obtainment of 40 bar of CO_2 pressure and 110 °C [18, 27, 34, 36]. Yet, reactions were performed using the same amount (in moles of ILs) contained in SX-EMIM MSO_3 4 and SX-BMIM Cl 4, and the same amount in grams of SX-Pristine (Table 1, entries 1–3, respectively).

The ^{1}H and ^{13} NMR analysis were performed on the final product of the reaction in which the SX-EMIM MSO_3 4 was used as a catalyst evidencing only propylene carbonate σ (ppm) signals: 1.5 (3H) and 19.4 (C) for CH_3 (methyl), 4.0 (1H), 4.6 (1H) and 74.9 (C) for CH_2 (methylene), 4.9 (1H) and 67.5 (C) for CH (methino) and 155.5 (C) for CO (carbonyl) [57, 58]. This result suggests that the catalyst was completely separated from the reaction product, by simple filtration. Yet, it must be emphasized that this catalyst showed a high selectivity (>99%, Table 1, entry 10) in the PC obtainment reaction.

Reactions were also performed only with ILs BMIM Cl and EMIM MSO_3 (Table 1, entries 1 and 2 respectively) in the same quantities presented in SX-BMIM Cl 4 and SX-EMIM MSO_3 4 (Table 1, entries 12 and 18 respectively). For both cases, there is an increase in PC conversion when ILs are supported in the SX matrix. It can be seen that when IL EMIM MSO_3 was used alone, only traces of PC were converted, and when it was supported in SX the PC conversion was 92.3%. This improvement in the behavior of ILs, when supported in SX, is probably due to the increase of the IL/gas interface (by spreading the IL on the support) as well as to the possibility of forming a thin layer of IL in the solid material helping to overcome problems such as the low mass transfer rate due to the ILs high viscosity [51, 59]. Yet, literature points out that the synergistic effect between nucleophilic anions, hydroxyl groups, and basic sites, present in SX-ILs facilitate the opening of the epoxide ring and CO_2 molecule insertion [60]. The results obtained in this work for PC synthesis using SX-ILs were auspicious when comparing with literature findings using as catalyst imidazolium-based ILs immobilized or functionalized in mesoporous silica. For instance, imidazolium-based ILs were grafted onto MCM-41 derived from rice husk and tested as catalysts in PC synthesis. The yield for the reaction was 68.8% (reaction conditions 150 °C and pressure of 15 bar of CO_2) [61]. Imidazolium-based ILs were immobilized on silica by a sol-gel method and used as a catalyst for PC synthesis in combination with $ZnCl_2$ (as co-catalyst). To obtain CP yield values higher than those presented in this work (91.4% CP) it was used approximately six times more ILs (96% CP) [62]. Finally, the catalyst was washed with acetone, filtered and dried at 60 °C in an oven, being reused three times until it lost more than 63% of its catalytic activity capacity.

To observe the performance of the SX-EMIM MSO_3 4 catalyst in reactions using different substrates, propylene epoxide was replaced by butylene epoxide and epichlorohydrin under the ideal conditions (40 bar, 110 °C and 6 h) previously determined for the synthesis of propylene carbonate. The conversions were 77% and 87% respectively, demonstrating the SX-EMIM MSO_3 4 potential to be used as an efficient catalyst for the synthesis of other cyclic carbonates.

4 Conclusion

Xerogel silicas containing 5% by weight (SX-ILs-1) of different imidazolium ionic liquids (BMIM Cl, BMIM NTf_2, MBMIM NTf_2, EMIM NTf_2, EMIM MSO_3 and EMIM CF_3SO_3) were tested as catalysts in the synthesis of propylene carbonate from the cycloaddition reaction of CO_2 in propylene epoxide. The two SX-ILs-1 with greater yield for these reactions were elected to study the effect of the increasing IL mass load (10%, 15%, 20% and 25%) in obtaining SX. It was observed that the increase in the load of the EMIM MSO_3 and BMIM Cl ILs increases the yield of propylene carbonate from 24.5% to 91.4% for SX-EMIM MSO_3 and from 37.2% to 83.4% for SX-BMIM Cl. However, it was concluded that there is a maximum amount of ILs that can be used in the synthesis of SX-IL. Values higher than the ideal resulted in weakened materials with low catalytic activity. Finally, we can point out that SX-EMIM MSO_3 4 is a promising alternative for use as a solid catalyst of easy separation catalyst/product for cycloaddition reactions in forming PC.

Acknowledgements This study was financed in part by the Coordenação de Aperfeiçoamento de Pessoal de Nivel Superior—Brasil (CAPES)—Finance Code 001. Sandra Einloft thanks CNPq for research scholarship.

Compliance with ethical standards

Conflict of interest The authors declare that there is no conflict of interest.

References

1. Chaugule AA, Bandhal HA, Tamboli AH et al (2016) Highly efficient synthesis of dimethyl carbonate from methanol and carbon dioxide using IL/DBU/SmOCl as a novel ternary catalytic system. Catal Commun 75:87–91. https://doi.org/10.1016/j.catcom.2015.12.009
2. Jiang X, Wang X, Nie X et al (2018) CO_2 hydrogenation to methanol on Pd-Cu bimetallic catalysts: H_2/CO_2 ratio dependence and surface species. Catal Today 316:62–70. https://doi.org/10.1016/j.cattod.2018.02.055
3. Roshan KR, Jose T, Kathalikkattil AC et al (2013) Microwave synthesized quaternized celluloses for cyclic carbonate synthesis from carbon dioxide and epoxides. Appl Catal A Gen 467:17–25. https://doi.org/10.1016/j.apcata.2013.07.007
4. Sreedhar I, Aniruddha R, Malik S (2019) Carbon capture using amine modified porous carbons derived from starch (Starbons®). SN Appl Sci 1:1–11. https://doi.org/10.1007/s42452-019-0482-8
5. Aresta M, Dibenedetto A, Angelini A (2013) The changing paradigm in CO_2 utilization. J CO2 Util 3–4:65–73. https://doi.org/10.1016/j.jcou.2013.08.001
6. Hui D, Fan N, Wang Y et al (2016) Recent advances in metal – free catalysts for the synthesis of cyclic carbonates from CO_2 and epoxides. Chin J Catal 37:826–845. https://doi.org/10.1016/S1872-2067(15)61085-3
7. Kathalikkattil AC, Roshan R, Tharun J et al (2016) A sustainable protocol for the facile synthesis of zinc-glutamate MOF: an efficient catalyst for room temperature CO_2 fixation reactions under wet conditions. Chem Commun 52:280–283. https://doi.org/10.1039/c5cc07781h
8. Klaus S, Lehenmeier MW, Anderson CE, Rieger B (2011) Recent advances in CO_2/epoxide copolymerization—new strategies and cooperative mechanisms. Coord Chem Rev 255:1460–1479. https://doi.org/10.1016/j.ccr.2010.12.002
9. Yang ZZ, He LN, Gao J et al (2012) Carbon dioxide utilization with C–N bond formation: carbon dioxide capture and subsequent conversion. Energy Environ Sci 5:6602–6639. https://doi.org/10.1039/c2ee02774g
10. Comès A, Fiorilli S, Aprile C (2020) Multifunctional heterogeneous catalysts highly performing in the conversion of carbon dioxide: mechanistic insights. J CO2 Util 37:213–221. https://doi.org/10.1016/j.jcou.2019.12.008
11. Alvaro M, Baleizao C, Carbonell E, Ghoul E (2005) Polymer-bound aluminium salen complex as reusable catalysts for CO_2 insertion into epoxides. Tetrahedron 61:12131–12139. https://doi.org/10.1016/j.tet.2005.07.114
12. Aresta M, Dibenedetto A, Gianfrate L, Pastore C (2003) Nb(V) compounds as epoxides carboxylation catalysts: the role of the solvent. J Mol Catal A Chem 205:245–252. https://doi.org/10.1016/S1381-1169(03)00305-4
13. Barbarini A, Maggi R, Mazzacani A, Mori G (2003) Cycloaddition of CO_2 to epoxides over both homogeneous and silica-supported guanidine catalysts. Tetrahedron Lett 44:2931–2934
14. Calabrese C, Liotta LF, Giacalone F, Gruttadauria M, Aprile C (2019) Supported polyhedral oligomeric silsesquioxane-based (POSS) materials as highly active organocatalysts for the conversion of CO_2. ChemCatChem 11(1):560–567. https://doi.org/10.1002/cctc.201801351
15. Chen A, Chen C, Xiu Y et al (2015a) Niobate salts of organic base catalyzed chemical fixation of carbon dioxide with epoxides to form cyclic carbonates†. Green Chem 17:1842–1852. https://doi.org/10.1039/c4gc02244k
16. Gao J, Song Q, He L et al (2012) Preparation of polystyrene-supported Lewis acidic Fe(III) ionic liquid and its application in catalytic conversion of carbon dioxide. Tetrahedron 68:3835–3842. https://doi.org/10.1016/j.tet.2012.03.048
17. Jutz F, Grunwaldt J, Baiker A (2008) Mn(III)(salen)-catalyzed synthesis of cyclic organic carbonates from propylene and styrene oxide in "supercritical" CO_2. J Mol Catal A Chem 279:94–103. https://doi.org/10.1016/j.molcata.2007.10.010
18. Shi TY, Wang JQ, Sun J et al (2013) Efficient fixation of CO_2 into cyclic carbonates catalyzed by hydroxyl-functionalized poly(ionic liquids). RSC Adv 3:3726–3732. https://doi.org/10.1039/c3ra21872d
19. Bresciani G, Bortoluzzi M, Marchetti F, Pampaloni G (2018) Iron(III)N, N-dialkylcarbamate-catalyzed formation of cyclic carbonates from CO_2 and epoxides under ambient conditions by dynamic CO_2 trapping as carbamato ligands. ChemSusChem 11(16):2737–2743. https://doi.org/10.1002/cssc.201801065
20. Buckley BR, Patel AP, Wijayantha KGU (2011) Electrosynthesis of cyclic carbonates from epoxides and atmospheric pressure carbon dioxide. Chem Comm 43:11888–11890. https://doi.org/10.1039/c1cc15467b
21. Guo Z, Jiang Q, Shi Y et al (2017) Tethering dual hydroxyls into mesoporous poly(ionic liquid)s for chemical fixation of CO_2 at ambient conditions: a combined experimental and theoretical study. ACS Catal 7:6770–6780. https://doi.org/10.1021/acscatal.7b02399
22. Meléndez J, North M, Pasquale R (2007) Synthesis of cyclic carbonates from atmospheric pressure carbon dioxide using exceptionally active aluminium (salen) complexes as catalysts.

Eur J Inorg Chem 21:3323–3326. https://doi.org/10.1002/ejic.200700521
23. Motokura K, Itagaki S, Iwasawa Y, Baba T (2009) Silica-supported aminopyridinium halides for catalytic transformations of epoxides to cyclic carbonates under atmospheric pressure of carbon dioxide. Green Chem 11:1876–1880. https://doi.org/10.1039/b916764c
24. Sun Q, Jin Y, Aguila B et al (2017) Porous ionic polymers as a robust and efficient platform for capture and chemical fixation of atmospheric CO_2. ChemSusChem 10:1160–1165. https://doi.org/10.1002/cssc.201601350
25. Toda Y, Komiyama Y, Kikuchi A, Suga H (2016) Tetraarylphosphonium salt-catalyzed carbon dioxide fixation at atmospheric pressure for the synthesis of cyclic carbonates. ACS Catal 6(10):6906–6910. https://doi.org/10.1021/acscatal.6b02265
26. Zhi Y, Shao P, Feng X et al (2018) Covalent organic frameworks: efficient, metal-free, heterogeneous organocatalysts for chemical fixation of CO_2 under mild conditions. J Mater Chem A 6:374–382. https://doi.org/10.1039/c7ta08629f
27. Aquino AS, Bernard FL, Vieira MO et al (2014) A new approach to CO_2 capture and conversion using imidazolium based-ionic liquids as sorbent and catalyst. J Braz Chem Soc 25:2251–2257. https://doi.org/10.5935/0103-5053.20140176
28. Bobbink FD, Dyson PJ (2016) Synthesis of carbonates and related compounds incorporating CO_2 using ionic liquid-type catalysts: state-of-the-art and beyond. J Catal 343:52–61. https://doi.org/10.1016/j.jcat.2016.02.033
29. Liang J, Chen RP, Wang XY et al (2017) Postsynthetic ionization of an imidazole-containing metal-organic framework for the cycloaddition of carbon dioxide and epoxides. Chem Sci 8:1570–1575. https://doi.org/10.1039/c6sc04357g
30. Liu X, Zhang S, Song QW et al (2016) Cooperative calcium-based catalysis with 1,8-diazabicyclo[5.4.0]-undec-7-ene for the cycloaddition of epoxides with CO_2 at atmospheric pressure. Green Chem 18:2871–2876. https://doi.org/10.1039/c5gc02761f
31. Maeda C, Taniguchi T, Ogawa K, Ema T (2015) Bifunctional catalysts based on m-phenylene-bridged porphyrin dimer and trimer platforms: synthesis of cyclic carbonates from carbon dioxide and epoxides. Angew Chem Int Ed 54:134–138. https://doi.org/10.1002/anie.201409729
32. Xiao L, Lv D, Wu W (2011) Brønsted acidic ionic liquids mediated metallic salts catalytic system for the chemical fixation of carbon dioxide to form cyclic carbonates. Catal Lett 141:1838–1844. https://doi.org/10.1007/s10562-011-0682-3
33. Saptal VB, Bhanage BM (2017) Current advances in heterogeneous catalysts for the synthesis of cyclic carbonates from carbon dioxide. Curr Opin Green Sust Chem 3:1–10. https://doi.org/10.1016/j.cogsc.2016.10.006
34. Rojas MF, Bernard FL, Aquino A et al (2014) Poly(ionic liquid)s as efficient catalyst in transformation of CO_2 to cyclic carbonate. J Mol Catal A Chem 392:83–88. https://doi.org/10.1016/j.molcata.2014.05.007
35. Kohrt C, Werner T (2015) Recyclable bifunctional polystyrene and silica gel-supported organocatalyst for the coupling of CO_2 with epoxides. ChemSusChem 8:2031–2034. https://doi.org/10.1002/cssc.201500128
36. Rodrigues DM, Hunter LG, Bernard FL et al (2019) Harnessing CO_2 into carbonates using heterogeneous waste derivative cellulose-based poly(ionic liquids) as catalysts. Catal Lett 149:733–743. https://doi.org/10.1007/s10562-018-2637-4
37. Barbosa AS, Lisboa JA, Silva MAO et al (2016) The novel Mesoporous silica aerogel modified with protic ionic liquid for lipase immobilization. Quim Nova 39:415–422. https://doi.org/10.5935/0100-4042.20160042
38. Donato RK, Migliorini MV, Benvegnu MA et al (2009) Synthesis of silica xerogels with highly distinct morphologies in the presence of imidazolium ionic liquids. J Sol-Gel Sci Technol 49:71–77. https://doi.org/10.1007/s10971-008-1829-6
39. Ott LS, Finke RG (2007) Transition-metal nanocluster stabilization for catalysis: a critical review of ranking methods and putative stabilizers. Coord Chem Rev 251:1075–1100. https://doi.org/10.1016/j.ccr.2006.08.016
40. Çok SS, Koç F, Balkan F, Gizli N (2019a) Revealing the pore characteristics and physicochemical properties of silica ionogels based on different sol-gel drying strategies. J Solid State Chem 278:120877. https://doi.org/10.1016/j.jssc.2019.07.038
41. Taubert A (2005) Inorganic materials synthesis – a bright future for ionic liquids? Acta Chim Slov 52:183–186
42. Fidalgo A, Ilharco LM (2004) Chemical tailoring of porous silica xerogels: local structure by vibrational spectroscopy. Chem Eur J 10:392–398. https://doi.org/10.1002/chem.200305079
43. dos Santos LM, Bernard FL, Polesso BB et al (2020) Designing silica xerogels containing RTIL for CO_2 capture and CO_2/CH_4 separation: influence of ILs anion, cation and cation side alkyl chain length and ramification. J Environ Manag 268:110340. https://doi.org/10.1016/j.jenvman.2020.110340
44. Dupont J, Consorti CS, Suarez PAZ, de Souza RF (2002) Preparation of 1-butyl-3-methyl imidazolium-based room temperature ionic liquids. Org Synth 79:236. https://doi.org/10.15227/orgsyn.079.0236
45. dos Santos LM, Ligabue R, Dumas A et al (2018) Waterborne polyurethane/Fe_3O_4-synthetic talc composites: synthesis, characterization, and magnetic properties. Polym Bull 75:1915–1930. https://doi.org/10.1007/s00289-017-2133-9
46. Barczak M, Borowski P (2019) Silica xerogels modified with amine groups: influence of synthesis parameters on porous structure and sorption properties. Microporous Mesoporous Mater 281:32–43. https://doi.org/10.1016/j.micromeso.2019.02.032
47. Zhang QG, Wang NN, Y ZW (2010) The hydrogen bonding interactions between the ionic liquid 1-ethyl-3-methylimidazolium ethyl sulfate and water. J Phys Chem B 114:4747–4754. https://doi.org/10.1021/jp1009498
48. Meera KMS, Sankar RM, Jaisankar SN, Mandal AB (2011) Mesoporous and biocompatible surface active silica aerogel synthesis using choline formate ionic liquid. Colloids Surf B: Biointerfaces 86:292–297. https://doi.org/10.1016/j.colsurfb.2011.04.011
49. Klingshirn MA, Spear SK, Holbrey JD, Rogers RD (2005) Ionic liquids as solvent and solvent additives for the synthesis of sol-gel materials. J Mater Chem 15:5174–5180. https://doi.org/10.1039/b508927a
50. Mirzaei M, Badiei AR, Mokhtarani B, Sharifi A (2017) Experimental study on CO_2 sorption capacity of the neat and porous silica supported ionic liquids and the effect of water content of flue gas. J Mol Liq 232:462–470. https://doi.org/10.1016/j.molliq.2017.02.104
51. Zhu J, He B, Huang J et al (2018) Effect of immobilization methods and the pore structure on CO_2 separation performance in silica-supported ionic liquids. Microporous Mesoporous Mater 260:190–200. https://doi.org/10.1016/j.micromeso.2017.10.035
52. Çok SS, Koç F, Balkan F, Gizli N (2019b) Exploring a new preparation pathway for the synthesis of silica based xerogels as crack-free monoliths. Ceram Int 45:1616–1626. https://doi.org/10.1016/j.ceramint.2018.10.038
53. Singh MP, Singh RK, Chandra S (2011) Studies on imidazolium-based ionic liquids having a large anion confined in a nanoporous silica gel matrix. J Phys Chem B 115:7505–7514. https://doi.org/10.1021/jp2003358

54. Karout A, Pierre AC (2007) Silica xerogels and aerogels synthesized with ionic liquids. J Non-Cryst Solids 353:2900–2909. https://doi.org/10.1016/j.jnoncrysol.2007.06.024
55. Chen Q, Peng C, Xie H et al (2015b) Cellulosic poly(ionic liquid)s: synthesis, characterization and application in the cycloaddition of CO_2 to epoxides. RSC Adv 5:44598–44603. https://doi.org/10.1039/c5ra05667e
56. Ivanova M, Kareth S, Petermann M (2018) Supercritical carbon dioxide and imidazolium based ionic liquids applied during the sol–gel process as suitable candidates for the replacement of classical organic solvents. J Supercrit Fluids 132:76–82. https://doi.org/10.1016/j.supflu.2017.07.005
57. Jia F, Chen X, Zheng Y et al (2015) One-pot atom-efficient synthesis of bio-renewable polyesters and cyclic carbonates through tandem catalysis. Chem Commun 51:8504–8507. https://doi.org/10.1039/c5cc01329a
58. Mandal M, Monkowius U, Chakraborty D (2016) Synthesis and structural characterization of titanium and zirconium complexes containing half-salen ligands as catalysts for polymerization reactions. New J Chem 40:9824–9839. https://doi.org/10.1039/c6nj02148d
59. Xin B, Hao J (2014) Imidazolium-based ionic liquids grafted on solid surfaces. Chem Soc Rev 43:7171–7187. https://doi.org/10.1039/c4cs00172a
60. Lan DH, Gong YX, Tan NY et al (2018) Multi-functionalization of GO with multi-cationic ILs as high efficient metal-free catalyst for CO_2 cycloaddition under mild conditions. Carbon 127:245–254
61. Muniandy L, Adam F, Rahman NRA, Ng EP (2019) Highly selective synthesis of cyclic carbonates via solvent free cycloaddition of CO_2 and epoxides using ionic liquid grafted on rice husk derived MCM-41. Inorg Chem Commun 104:1–7. https://doi.org/10.1016/j.inoche.2019.03.012
62. Xiao L, Li F, Peng J, Xia C (2006) Immobilized ionic liquid/zinc chloride: heterogeneous catalyst for synthesis of cyclic carbonates from carbon dioxide and epoxides. J Mol Catal A Chem 253:265–269. https://doi.org/10.1016/j.molcata.2006.03.047